

Phase-Based Signal Representations for Scattering

1st Daniel Haider
Acoustics Research Institute
Austrian Academy of Sciences
Vienna, Austria
daniel.haider@oeaw.ac.at

2nd Peter Balazs
Acoustics Research Institute
Austrian Academy of Sciences
Vienna, Austria
peter.balazs@oeaw.ac.at

3rd Nicki Holighaus
Acoustics Research Institute
Austrian Academy of Sciences
Vienna, Austria
nicki.holighaus@oeaw.ac.at

Abstract—The scattering transform is a non-linear signal representation method based on cascaded wavelet transform magnitudes. In this paper we introduce phase scattering, a novel approach where we use phase derivatives in a scattering procedure. We first revisit phase-related concepts for representing time-frequency information of audio signals, in particular, the partial derivatives of the phase in the time-frequency domain. By putting analytical and numerical results in a new light, we set the basis to extend the phase-based representations to higher orders by means of a scattering transform, which leads to well localized signal representations of large-scale structures. All the ideas are introduced in a general way and then applied using the STFT.

I. Introduction

For most applications using time-frequency representations, only the magnitude of the obtained complex coefficients is considered as, e.g., in the cases of spectrogram and scalogram [1]. This is a standard method for analyzing the time-frequency content of an audio signal, which is also heavily used in deep learning for audio, where neural networks and time-frequency (magnitude) representations often go hand-in-hand [2]–[4]. In this context, the *scattering transform* provides an important link, as it may be interpreted as a deterministic neural network, computing a cascade of filter magnitude transformations, i.e. a sequence of filtering and application of the modulus as non-linearity. As signal representation, it is able to reveal large-scale structures of the signal [5], which is partly caused by the non-linearity, i.e. discarding the phase information. The phase is visually very unintuitive but its derivative in the time, as well as in the frequency direction yield very informative and intuitive phase-based signal representations. The resulting quantities overcome some of the issues of the (pure) phase and are directly linked to the concepts of *instantaneous frequency* and *group delay*. The interest of this work is to investigate the idea of scattering with a complementary approach as before, namely considering the partial derivatives of the phase instead of the modulus as non-linear step. As in the magnitude case, larger-scale structures can be revealed with this *phase scattering* procedure, additionally inheriting the precision of the localization of time-frequency information that is provided by these phase-based signal representations.

This work was supported by the Austrian Science Fund (FWF) START-project FLAME (Frames and Linear Operators for Acoustical Modeling and Parameter Estimation; Y 551-N13).

In Section II we revisit basic results around the concepts of *instantaneous frequency* and *group delay*, in particular a result related to the short-time Fourier transform (STFT). This revision shows the nature of the introduced concepts from a different perspective, which is the key for the main part of the paper. Analytical and numerical results are provided in order to strengthen the intuition. In Section III we start by briefly presenting the scattering transform in a time-frequency setting and adapt its principle structure to define the *phase scattering coefficients*. Finally we show promising experiments on proof-of-concept examples in a direct comparison to (magnitude) scattering based on the STFT. This first study sets the basis and intuition for further research on this idea.

The content of this paper was mainly developed in the Master’s thesis of the first author [6]. More details, including proofs and Matlab scripts are available under <https://github.com/danedane-haider/Phase-Scattering-Masterthesis>. The scripts use the LTFAT toolbox [7], [8].

II. Instantaneous Frequency and Group Delay

Instantaneous frequency (IF) and *group delay* (GD) are important concepts in signal analysis [1] as they provide precise information about frequency, resp. temporal positioning of signal components [9]. Local versions are defined by the partial derivatives of the phase in the time-frequency plane. Let $\Phi_{\Psi}^x(t, \omega)$ denote the phase function of a complex-valued time-frequency representation, based on a family of localization functions Ψ , then

$$\hat{\omega}_{\Psi}(x; t, \omega) = \frac{1}{2\pi} \frac{\partial}{\partial t} \Phi_{\Psi}^x(t, \omega) \quad (1)$$

is called *channelized instantaneous frequency* (CIF) and

$$\hat{\tau}_{\Psi}(x; t, \omega) = -\frac{\partial}{\partial \omega} \Phi_{\Psi}^x(t, \omega) \quad (2)$$

local group-delay (LGD) of x w.r.t. Ψ . These concepts have been used already many times, e.g. for the phase vocoder [10] or reassignment methods [11], [12] and other types of phase-based processing [13]. In this work we focus on the STFT as underlying time-frequency representation. According to the scaling conventions we use, its phase function $\Phi_g^x(t, \omega)$ using a window g is found in its magnitude-phase representation in the following way,

$$\mathcal{V}_g x(t, \omega) = |\mathcal{V}_g x(t, \omega)| \cdot e^{2\pi i \Phi_g^x(t, \omega)}. \quad (3)$$

Usually, when working with the STFT, a specific phase convention is assumed. The resulting phase can then be converted into a time-invariant and a frequency-invariant version. In contrast to previous work, we select specific invariances in the STFT beforehand for computing CIF and LGD respectively. For $x, g \in L^2(\mathbb{R})$ the *frequency-invariant* STFT is defined by

$$\mathcal{V}_g x(t, \omega) = \int_{\mathbb{R}} x(\tau) \overline{g(\tau - t)} e^{-2\pi i \omega \tau} d\tau, \quad (4)$$

$t, \omega \in \mathbb{R}$. Here, the exponential term is independent of the time index t . The *time-invariant* STFT is defined by changing the order of modulation and translation, giving

$$\mathcal{V}_g^t x(t, \omega) = \int_{\mathbb{R}} x(\tau) \overline{g(\tau - t)} e^{-2\pi i \omega (\tau - t)} d\tau. \quad (5)$$

Our approach is to consider CIF in a frequency-invariant (4) and LGD in a time-invariant setting (5). This results directly in modes of these quantities that are necessary for the last chapter of the paper. Note that this setting only agrees with the original definitions (1) and (2) up to the induced invariances. Therefore, we will use the notation CIF_f and LGD_t further on. The following proposition shows how CIF_f and LGD_t can be computed based on a result by Auger and Flandrin [11]. We additionally emphasize the formal requirements [14] and consider the introduced STFT-invariances (4) and (5).

Proposition 1. *Let $x \in L^2(\mathbb{R})$ and $g \in L^2(\mathbb{R}) \cap C^1(\mathbb{R})$, such that $Tg \in L^2(\mathbb{R})$, where the time-weighted window Tg is given by $Tg(\tau) = \tau g(\tau)$ for all $\tau \in \mathbb{R}$. Then $\mathcal{V}_g x(t, \omega)$ and $\mathcal{V}_g^t x(t, \omega)$ are infinitely partially differentiable in both variables, t and ω . Let further g' denote the differentiated window $g'(\tau) = \frac{d}{d\tau} g(\tau)$. Then, for $\mathcal{V}_g x(t, \omega) \neq 0$, CIF_f and LGD_t can be computed by*

$$\widehat{\omega}_{\text{STFT}}(x; t, \omega) = -\frac{1}{2\pi} \text{Im} \left\{ \frac{\mathcal{V}_{g'} x(t, \omega)}{\mathcal{V}_g x(t, \omega)} \right\} \quad (6)$$

$$\widehat{\tau}_{\text{STFT}}(x; t, \omega) = \text{Re} \left\{ \frac{\mathcal{V}_{Tg}^t x(t, \omega)}{\mathcal{V}_g^t x(t, \omega)} \right\}, \quad t, \omega \in \mathbb{R}. \quad (7)$$

A compact proof of this can be found in [6]. The impact of the STFT invariances gets clear in the following.

A. Analytical Shapes of CIF and LGD - Revisited

Based on Proposition 1, one finds the CIF_f of stationary sinusoids and the LGD_t of Dirac impulse to be affine linear functions. The results may be considered as known, however, they show an alternative point of view via the induced STFT-invariances which is crucial for the construction of the phase scattering coefficients in the last section.

1) *CIF_f Analytically:* The CIF_f representation of a stationary sinusoid (based on a frequency-invariant STFT) has linear behaviour along the frequency axis, centered at the IF of the sinusoid.

Lemma 1. *Let $x(\tau) = e^{2\pi i \xi_0 \tau}$ be a complex sinusoid with frequency ξ_0 and g a window function with $g, Tg \in L^2(\mathbb{R}) \cap L^1(\mathbb{R})$ such that the Fourier transform of g has no zeros and*

the Fourier transform of Tg only a single one at 0. Then Equation (6) reduces to

$$\widehat{\omega}_{\text{STFT}}(x; t, \omega) = \xi_0 - \omega \quad (8)$$

$t, \omega \in \mathbb{R}$.

Note that using a time-invariant STFT results in $\widehat{\omega}_{\text{STFT}}(x; t, \omega) = \xi_0$, yielding the IF directly, whereas here a frequency shift function is computed, measuring the distance to ξ_0 linearly.

2) *LGD_t Analytically:* The LGD_t representation of a Dirac impulse (based on a time-invariant STFT) has linear behaviour along the time axis, centered at the impulse.

Lemma 2. *Let $x(\tau) = \delta(\cdot - \tau_0)$ where δ denotes a Dirac impulse and $g \in L^2(\mathbb{R}) \cap C^1$ with $g' \in L^2(\mathbb{R})$ where g has no zeros and g' only a single one at 0. Then Equation (7) reduces to*

$$\widehat{\tau}_{\text{STFT}}(x; t, \omega) = \tau_0 - t \quad (9)$$

$t, \omega \in \mathbb{R}$.

Also here, using the time-invariant version of the STFT is key to obtain this affine linear function and is not obtained when using the frequency-invariant STFT. The results of the Lemmata can be deduced directly from Proposition 1, see [6].

Thus, by choosing the specific STFT versions in this discriminative way, CIF_f and LGD_t are linear functions in frequency resp. time direction. We briefly illustrate this also numerically to strengthen the intuition.

B. Numerical Shapes of CIF and LGD - Revisited

Proposition 1 provides a convenient method to compute phase derivatives numerically by point-wise operations of two STFTs. However, when working with finitely supported windows in applications, the computations (6) and (7) clearly have to be restricted to the support of the window, i.e. CIF_f and LGD_t coefficients are considered to be zero outside the supports. Therefore, in an actual numerical representation the linear shapes from (8) and (9) are localized naturally to the range of the window support as well. Using the toy examples from Lemma 1 and 2 with $\xi_0 = 1000\text{Hz}$ and $\tau_0 = 0.5\text{s}$, one finds the piece-wise linearly decreasing functions locally around ξ_0 , resp. τ_0 . Figure 1 (a),(b) illustrates well how CIF_f and LGD_t resemble one another in terms of their shape in time, resp. frequency direction, emphasizing the duality of the two quantities. Panels (c),(d) show the direct comparisons to STFT magnitudes. Besides the intuition this brings for phase-based signal representations in general, the chosen STFT conventions allow to use CIF_f and LGD_t in a scattering procedure in a meaningful way.

For the calculation of the plots we used the function `gabphaserderiv` from the *Large Time-Frequency Toolbox* (LTFAT) [7] with the additional flags '`freqinv`' and '`timeinv`', which follow the STFT conventions used in Proposition 1, based on the discrete Gabor transform `dgt`. Discrete versions of a dilated Gaussian are used as window functions.

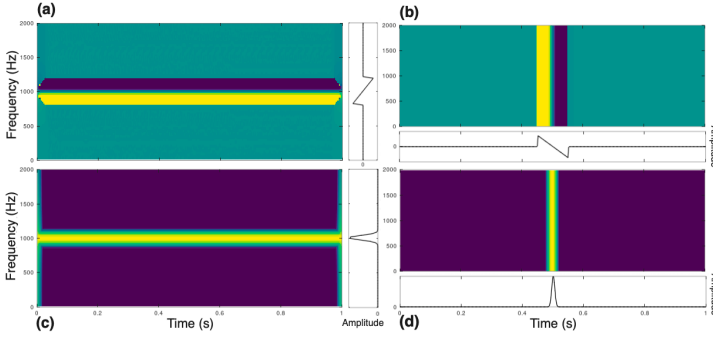


Figure 1: (a) Full CIF_f of sinusoid and one column for fixed t (right). (b) full LGD_t of impulse and one column for fixed ω (bottom). (c) full STFT magnitude of sinusoid and one column for fixed t (right). (d) full STFT magnitude of impulse and one column for fixed ω (bottom).

III. Phase Scattering

Indeed, the partial derivatives of the time-frequency domain phase are useful quantities for describing time-frequency information since they provide precise time and frequency localization of harmonic resp. transient events of a signal. Using the analytical results and the intuition from the previous section, we aim for expanding the representations to higher orders in the manner of the *scattering transform*.

A. Time-Frequency Scattering

The computational scheme of the scattering transform is a cascade of absolute values of filter transformations [15], [16]. A network-like structure emerges that results in layers of magnitude filter decompositions. In a time-frequency setting this can be seen as taking one set of localization functions (band-pass filters) per layer, applied via convolution (originally using wavelet filters). Several papers show this transform as promising tool to represent large-scale features of audio signals, such as amplitude or frequency modulation, chord structures (intervals), tempo and rhythm, etc. [17]–[19]. Therefore, it is often used as external feature extraction step for deep learning tasks and moreover, is celebrated as being an interpretable neural network itself with fixed filters and a solid mathematical foundation, allowing for rigorous analysis.

Definition 1 (Time-Frequency Scattering). *Let $x \in L^2(\mathbb{R})$ and $\Psi_k = \{\psi_i^k\}_{i \in \Lambda_k}$ denote the set of filters for the k -th layer. Λ_k is the corresponding (frequency-)index set and the operator $\mathcal{U}_k[p_0] = |\psi_{p_0} * \cdot|$ computes the magnitude filtering at index p_0 . Then, the scattering transform is a cascade of the operators $\mathcal{U}_1, \dots, \mathcal{U}_k$ along a frequency-index path $p = (p_1, \dots, p_k) \in \Lambda_1 \times \dots \times \Lambda_k$ and we call*

$$\mathcal{S}[p]x = \mathcal{U}_k[p_k] \dots \mathcal{U}_2[p_2] \mathcal{U}_1[p_1]x \quad (10)$$

the k -th order (magnitude) scattering coefficients w.r.t. p .

The original idea of the scattering transform was to create a translation-invariant representation on $L^2(\mathbb{R})$ by integrating over the emerging scattering coefficients [15]. In applications,

a final low-pass filtering step is used to simulate this property locally. In this work we preliminarily do not consider this step and focus merely on the nature of the coefficients.

B. CIF and LGD Scattering

Instead of taking the modulus of the complex time-frequency coefficients, we use the mappings to the partial derivatives of the phase as non-linearity in the scattering cascade. This procedure can be written in terms of operators, defined in the following way.

Definition 2 (Phase Scattering Coefficients). *Let $x \in L^2(\mathbb{R})$ and Ψ a family of localization functions with index set Λ , then the operators*

$$(\widehat{\Omega}_\Psi[p_0]x)(t) := \widehat{\omega}_\Psi(x; t, p_0) \quad (11)$$

$$(\widehat{T}_\Psi[p_0]x)(t) := \widehat{\tau}_\Psi(x; t, p_0) \quad (12)$$

compute CIF and LGD of x at the frequency index $p_0 \in \Lambda$ as function of time. Let $p = (p_1, \dots, p_k) \in \Lambda_1 \times \dots \times \Lambda_k$ denote a frequency-index path associated to k families of localization functions Ψ_1, \dots, Ψ_k , then cascading the operators (11) and (12) along p defines the k -th order CIF scattering coefficients

$$\widehat{\Omega}[p]x = \widehat{\Omega}_{\Psi_k}[p_k] \dots \widehat{\Omega}_{\Psi_1}[p_1]x \quad (13)$$

and the k -th order LGD scattering coefficients

$$\widehat{T}[p]x = \widehat{T}_{\Psi_k}[p_k] \dots \widehat{T}_{\Psi_1}[p_1]x. \quad (14)$$

of x w.r.t. p . We shall call $\widehat{\Omega}[(q_1, \dots, q_{k-1}, \lambda)]x$, considered for all $\lambda \in \Lambda_k$, the k -th CIF scattering layer of x w.r.t. the path $q = (q_1, \dots, q_{k-1})$. Analog for the LGD case.

Building on the results from the previous chapter, we use a phase scattering procedure that use CIF_f and LGD_f computed by the STFT to provide numerical examples.

Definition 3 (STFT-Phase Scattering Coefficients). *Under the conditions from Proposition 1 we can define the STFT-phase (or CIF_f resp. LGD_f) scattering coefficients analogously to (13) and (14) by cascading the operators*

$$(\widehat{\Omega}_{\text{STFT}}[p_0]x)(t) = -\frac{1}{2\pi} \text{Im} \left\{ \frac{\mathcal{V}_{g'}x(t, p_0)}{\mathcal{V}_g x(t, p_0)} \right\}, \quad (15)$$

$$(\widehat{T}_{\text{STFT}}[p_0]x)(t) = \text{Re} \left\{ \frac{\mathcal{V}_{Tg}^t x(t, p_0)}{\mathcal{V}_g^t x(t, p_0)} \right\}, \quad t \in \mathbb{R} \quad (16)$$

along a frequency-index path $p = (p_1, \dots, p_k) \in \mathbb{R}^k$, associated to k STFTs using windows g_1, \dots, g_k .

Inspired by the experiments from [17]–[19], we show that 2nd order phase scattering coefficients are capable of capturing wider scale information, comparable to magnitude scattering.

1) *CIF_f Scattering Application - Frequency Modulation:* We first show that CIF_f scattering of a frequency modulated sinusoid finds the modulation frequency in the 2nd layer.

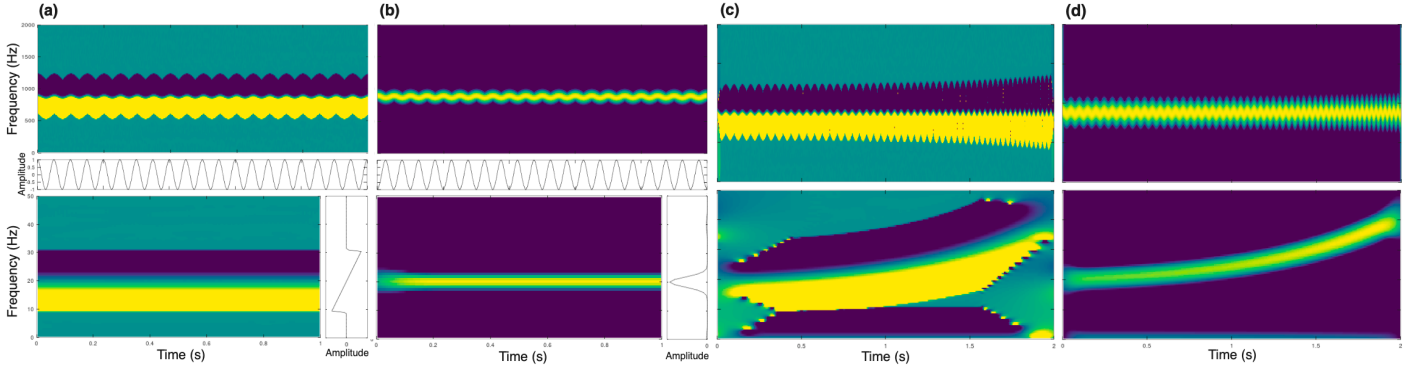


Figure 2: (a),(b) 1st and 2nd order CIF_f and STFT scattering layers of x_1 with propagation channel at 880Hz. (c),(d) 1st and 2nd order CIF_f and STFT scattering layers of x_2 .

Lemma 3. Let $x(\tau) = e^{2\pi i(\xi_0\tau + \gamma(\tau))}$ with $\gamma(\tau) = \sin(2\pi\xi_1\tau)$ denote a vibrato signal with center frequency ξ_0 and modulation frequency ξ_1 . Then the 2nd order CIF_f scattering layer of x w.r.t. $p_1 = \xi_0$ is given by

$$(\widehat{\Omega}_{\text{STFT}}[\xi_0, \omega]x)(t) = \xi_1 - \omega \quad (17)$$

$t, \omega \in \mathbb{R}$.

This result shows the natural extension of the (1st order) CIF_f representation from Lemma 1. Let $\phi(\tau)$ denote the temporal phase of x , given as above. We see that the instantaneous frequency of x is $\omega(x; \tau) = \frac{1}{2\pi} \frac{d}{d\tau} \phi(\tau) = \xi_0 + 2\pi\xi_1 \cos(2\pi\xi_1\tau)$, which when considered as a time-domain signal itself possesses the IF $\omega(\omega(x; \tau); \tau) = \xi_1$, the modulation frequency of the vibrato. Using 2nd order CIF_f scattering, we find ξ_1 as zero of an affine linear function, coming from $(\widehat{\Omega}_{\text{STFT}}[\omega]x)(t) = \omega(x; t) - \omega$. A more detailed discussion can be found in [6].

Note that this result theoretically does not depend on the chosen propagation index p_1 , however, in the numerical case we have to care about staying inside the support of the window, i.e. $p_1 \in \text{supp}(\widehat{g})$.

As numerical examples we set up two sinusoidal signals x_1, x_2 at 880Hz and modulate x_1 by $\gamma_1(\tau) = \sin(2\pi 20\tau)$, creating a constant vibrato of 20Hz and x_2 by $\gamma_2(\tau) = \sin(2\pi\tau(20 + e^\tau))$, creating a vibrato that increases exponentially in frequency, beginning at 20Hz. Figure 2 shows 1st and 2nd order CIF_f and STFT scattering layers of x_1 and x_2 , using the propagation frequency index corresponding to 880Hz. Although the modulation frequencies induced by γ_1 and γ_2 are extremely low, they are captured precisely in the 2nd CIF_f layers respectively as zeros of linear functions. This can be observed also for more general frequency modulation functions. Magnitude scattering finds the modulation frequencies as well, but here in terms of shifted window functions.

C. Mixed Phase Scattering

To provide an intuitive application of LGD scattering, we refer to an earlier work [19] where we have shown how STFT magnitude scattering can capture the frequency of temporal

patterns among transients in a signal. In this sense, our approach is to use the LGD_t representation as transient detector and use a subsequent CIF_f transformation to get the frequency information of the LGD_t -peak arrangement.

Definition 4 (Mixed Phase Scattering). Let $x \in L^2(\mathbb{R})$ and Ψ_1, Ψ_2 families of localization functions, then we define

$$\widehat{M}[p_1, p_2]x = \widehat{\Omega}_{\Psi_2}[p_2] \widehat{T}_{\Psi_1}[p_1]x \quad (18)$$

as 2nd order mixed phase scattering coefficients of x w.r.t. the path (p_1, p_2) .

1) *Mixed Phase Scattering Application - Dirac Comb:* We show that 2nd order mixed scattering finds the fundamental frequency of a Dirac comb signal.

Lemma 4. Let $x(\tau) = \sum_{\ell \in \mathbb{Z}} \delta(\cdot - \frac{2\pi\ell}{\xi_0})$ be a Dirac comb with fundamental frequency ξ_0 . Then the 2nd order mixed phase scattering layer of x is given by

$$(\widehat{M}[p_1, \omega]x)(t) = \xi_0 - \omega \quad (19)$$

for any p_1 and $t, \omega \in \mathbb{R}$.

Crucial for this result is to use a window g with $\text{supp}(g) \geq 2\pi/\xi_0$ to avoid regions of zero amplitude between the impulses. Then $(\widehat{T}_{\text{STFT}}[\omega]x)(t)$ is a saw-tooth wave for every $\omega \in \mathbb{R}$ with a fundamental frequency of ξ_0 and the same phase function as its sinusoidal equivalent, i.e. the IF is found by the subsequent CIF_f transformation analog to Lemma 3. A more detailed discussion can be found in [6]. Figure 3 shows the mixed phase scattering and STFT scattering layers of a Dirac comb signal with fundamental frequency of 20Hz.

IV. Conclusion and Outlook

We revisited channelized instantaneous frequency and local group delay by pointing out their linear characters when considering two different STFT-invariance settings. Analytical and numerical arguments are provided in order to emphasize this perspective. Based on that we introduced an extension of these representations in the manner of the scattering transform by cascading the computations, called *phase scattering*. It

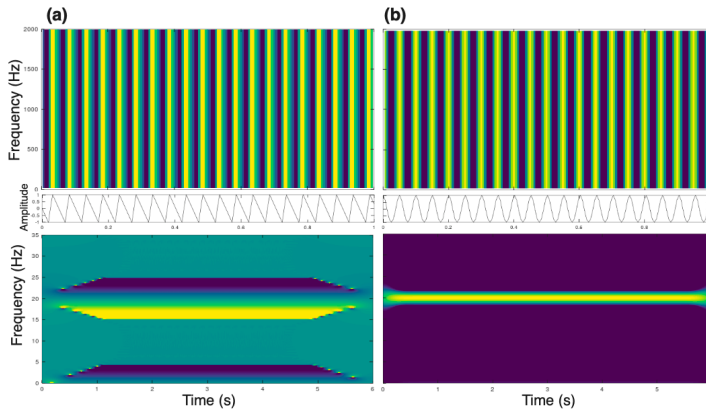


Figure 3: (a) 1st and 2nd order mixed phase scattering layers of the Dirac comb w.r.t. an arbitrary p_1 . (b) 1st and 2nd order STFT scattering layers.

turned out that this procedure is, like the original scattering, capable of extracting information that lives in larger scales. We found modulation frequencies of vibrato signals and the tempo of a Dirac comb emerging in the second layer of the transform. However, other than the blurred representation of time-frequency information that magnitude scattering provides, CIF_T and LGD_T scattering allows for precise allocation of large-scale time-frequency information by means of zeros of linear functions.

This first study provides the foundation and intuition for further investigations on scattering phase information. The many existing results related to the scattering transform may serve as source of inspiration. In particular, to provide a mathematically well-defined setting one could formulate phase scattering in terms of distribution theory. Then, the expected properties regarding translation-invariance could be approached in theory. An immediate next step for continuing numerical experiments should be the development of computational algorithms that produce clean plots and further on, how phase scattering performs on real world audio signals. Finally, given the precise allocation properties, it seems promising to evaluate a set of phase-based scattering features as pre-processing step for a classification task.

Acknowledgment

The work on this paper was partially supported by the Austrian Science Fund (FWF) START-project FLAME (Frames and Linear Operators for Acoustical Modeling and Parameter Estimation; Y 551-N13) and MERLIN (I 3067-N30).

References

- [1] P. Flandrin, *Time-Frequency/Time-Scale Analysis*, Academic Press, San Diego, 1999.
- [2] A. Marafioti, P. Majdak, N. Holighaus, and N. Perraudin, “GACELA: A generative adversarial context encoder for long audio inpainting of music,” *IEEE Journal of Selected Topics in Signal Processing*, vol. 15, no. 1, pp. 120–131, 2021.
- [3] F. Huang and P. Balazs, “Harmonic-aligned frame mask based on non-stationary Gabor transform with application to content-dependent speaker comparison,” in *Proceedings of Interspeech 2019*, 2019, pp. 151–155.

- [4] H. Purwins, B. Li, T. Virtanen, J. Schlüter, S. Chang, and T. Sainath, “Deep learning for audio signal processing,” *IEEE Journal of Selected Topics in Signal Processing*, vol. 13, no. 2, pp. 206–219, 2019.
- [5] R. Bammer, M. Dörfler, and P. Harar, “Gabor frames and deep scattering networks in audio processing,” *Axioms*, vol. 8, no. 4, art. 106, 2019.
- [6] D. Haider, “Aspects of time-frequency scattering and towards phase scattering,” M.S. thesis, University of Vienna, 2019.
- [7] P. Søndergaard, B. Torrèsani, and P. Balazs, “The linear time frequency analysis toolbox,” *International Journal of Wavelets, Multiresolution and Information Processing*, vol. 10, no. 4, 1250032, 2012.
- [8] Z. Průša, P. Søndergaard, N. Holighaus, C. Wiesmeyer, and P. Balazs, “The Large Time-Frequency Analysis Toolbox 2.0,” in *Sound, Music, and Motion*, M. Aramaki, O. Derrien, R. Kronland-Martinet, and S. Ystad, Eds., Lecture Notes in Computer Science, pp. 419–442. Springer, 2014.
- [9] S. Mallat, *A Wavelet Tour of Signal Processing - The Sparse Way*, Academic Press, 2009.
- [10] M. Dolson, “The phase vocoder: A tutorial,” *Computer Musical Journal*, vol. 10, no. 4, pp. 11–27, 1986.
- [11] P. Flandrin, F. Auger, and E. Chassande-Mottin, “Time-frequency reassignment: From principles to algorithms,” *Applications in Time-Frequency Signal Processing*, p. 179–203, 2003.
- [12] N. Holighaus, Z. Průša, and P. Søndergaard, “Reassignment and synchrosqueezing for general time-frequency filter banks, subsampling and processing,” *Signal Processing* 125, pp. 1–8, 2016.
- [13] T. Gerkmann, M. Krawczyk-Becker, and J. Le Roux, “Phase processing for single-channel speech enhancement: History and recent advances,” *IEEE Signal Processing Magazine*, vol. 32, no. 2, pp. 55–66, 2015.
- [14] P. Balazs, D. Bayer, F. Jaillet, and P. Søndergaard, “The phase derivative around zeros of the short-time Fourier transform,” *Applied and Computational Harmonic Analysis*, vol. 30, no. 3, pp. 610–621, 2016.
- [15] S. Mallat, “Group invariant scattering,” *Communications on Pure and Applied Mathematics*, vol. 65, no. 10, pp. 1331–1398, 2012.
- [16] T. Wiatowski and H. Bölcskei, “Deep neural networks based on semi-discrete frames,” in *Proceedings of the IEEE International Symposium on Information Theory (ISIT)*, 2015, pp. 1212–1216.
- [17] J. Andén and S. Mallat, “Deep scattering spectrum,” *IEEE Transactions on Signal Processing*, vol. 62, no. 16, pp. 4114–4128, 2014.
- [18] R. Bammer and M. Dörfler, “Invariance and stability of Gabor scattering for music signals,” in *Proceedings of Sampling Theory and Applications (SampTA)*, 2017, pp. 299–302.
- [19] D. Haider and P. Balazs, “Extraction of rhythmical features with the Gabor scattering transform,” in *Proceedings of the 14th International Symposium on Computer Music Multidisciplinary Research (CMMR)*, 2019, pp. 916–923.